

## Accepted Manuscript

Virtual calculation of the B-value allowables of notched composite laminates

O. Vallmajó, I.R. Cozar, C. Furtado, R. Tavares, A. Arteiro, A. Turon, P.P. Camanho

PII: S0263-8223(18)34531-8

DOI: <https://doi.org/10.1016/j.compstruct.2018.12.049>

Reference: COST 10512

To appear in: *Composite Structures*

Received Date: 14 December 2018

Accepted Date: 19 December 2018



Please cite this article as: Vallmajó, O., Cozar, I.R., Furtado, C., Tavares, R., Arteiro, A., Turon, A., Camanho, P.P., Virtual calculation of the B-value allowables of notched composite laminates, *Composite Structures* (2018), doi: <https://doi.org/10.1016/j.compstruct.2018.12.049>

This is a PDF file of an unedited manuscript that has been accepted for publication. As a service to our customers we are providing this early version of the manuscript. The manuscript will undergo copyediting, typesetting, and review of the resulting proof before it is published in its final form. Please note that during the production process errors may be discovered which could affect the content, and all legal disclaimers that apply to the journal pertain.

## Virtual calculation of the B-value allowables of notched composite laminates

O. Vallmajó<sup>a</sup>, I.R. Cozar<sup>a</sup>, C. Furtado<sup>b,c</sup>, R. Tavares<sup>a,b,c</sup>, A. Arteiro<sup>b,c</sup>, A. Turon<sup>a,\*</sup>, P. P. Camanho<sup>b,c</sup>

<sup>a</sup> AMADE, Polytechnic School, University of Girona, C/Universitat de Girona 4, 17003 Girona, Spain

<sup>b</sup> DEMec, Faculdade de Engenharia, Universidade do Porto, Rua Dr. Roberto Frias, 4200-465 Porto, Portugal

<sup>c</sup> INEGI, Rua Dr. Roberto Frias, 400, 4200-465 Porto, Portugal

---

**Abstract**

The design of composite structures relies on the accurate determination of design allowables, which are statistically based material parameters that take into account manufacturing, geometrical and microstructure variability. The accurate determination of these design parameters requires extensive experimental testing, which makes the certification process of a composite material extremely costly and time consuming. To increase the efficiency of the design process, there is the need to develop alternatives to the mostly experimental material characterization process, ideally based on accurate and quick modelling analysis combined with powerful statistical tools.

In this work an analytical model to compute the notched strength of composite structures based on three ply-based material properties (elastic modulus, unnotched strength and  $\mathcal{R}$ -curve) is combined with an uncertainty quantification and management (UQ&M) framework to compute the B-basis design allowables of notched configurations of CFRP laminates. The framework is validated with open-hole tension experimental results for the IM7/8552 material. Given the analytical nature of the developed framework and consequent computational efficiency, the UQ&M methodology is applied to the generation of design charts for notched geometries, whose generation would otherwise be impractical, using experimental test based methods.

---

\*Corresponding author. Tel.: +34 972 418 492

Email address: albert.turon@udg.edu (A. Turon)

## 1. Introduction

The design and certification of composite structures is based on the building block approach [1]. This approach relies on the accurate determination of design allowables that drive the design of structures at larger scales. These design allowables are statistically based material parameters that define an acceptable stress value for a material and, therefore, ensure their safe and efficient use. Design allowables have to account for the variability of the material properties and of the manufacturing process, and are a function of the structural details and loading conditions [2] and, consequently, their experimental determination is an extremely costly and time-consuming process. The standard design allowable used in the aeronautical industry for fail safe structures is the B-basis [1, 3], which is defined as the 95% lower confidence bound on the tenth percentile of a specified population of measurements. This is a conservative allowable that ensures with 95% confidence that 90% of the population will have a given property, e.g. strength, higher than the B-value allowable.

It is of key importance to accurately determine these design allowables, however, time consuming processes are not ideal during preliminary design. For this reason, alternatives to fully experimental material characterization have been proposed, namely, the use of statistically based numerical and analytical models [4, 5, 6, 3]. These models include the influence of the uncertainty related to the determination of the input parameters and their intrinsic variability on the global response of the model. A convenient way to describe these uncertain quantities is to describe them using a probability distribution which can be defined through experimental measurements or assumed based on empirical evidence.

The stochastic finite element method [7, 5] is a powerful tool to address the influence of the uncertainty related to the determination of the material and geometrical properties and loading conditions on the global response of composite structures. Nam et al. [7] proposed a methodology to determine the design allowables of composite laminates using lamina level test data and finite element analysis and validate the proposed methodology for both un-notched and open hole strength. However, stochastic finite element method solutions rely on computationally expensive procedures, which makes the consideration of the variability of the input parameters an extremely time consuming and, therefore, impracticable process quick design.

Quick analytical prediction tools are therefore desirable, specially for preliminary design and material selection. Furtado et al. [8] proposed an analytical framework to estimate the notched strength of multi-directional carbon-epoxy laminates based on three ply properties (the longitudinal Young's modulus, the longitudinal strength, and the longitudinal crack resistance curve) and concluded that the framework was able to provide good predictions for the open-hole tensile and compressive strengths of general balanced carbon/epoxy laminates. Since the model uses ply-level properties as building blocks, it is ideal for preliminary design, since the notched strength of different layups and geometries can be quickly estimated.

The authors validated the analytical framework for the nominal values of the material properties and

the geometrical parameters. However, the uncertainty associated to the material properties and dimensions may be taken into account in an attempt to define design allowables for the notched strength.

In this work, a methodology to predict the B-value of notched composite laminates using the analytical framework proposed by Furtado et al. [8] is proposed by taking the variability of the material properties that dominate failure and the effect of geometrical imperfections into account. The proposed Uncertainty Quantification and Management (UQ&M) methodology is validated against available experimental data and is applied to generate practical engineering design tools.

## 2. Methodology

### 2.1. Description of the analytical framework

Furtado et al. [8] proposed an analytical framework to estimate the notched strength of multidirectional carbon-epoxy laminates based on three ply properties: the longitudinal Young's modulus,  $E_1$ , the longitudinal strength,  $X$ , and the longitudinal crack resistance curve,  $\mathcal{R}$ -curve. The framework combines the finite fracture mechanics model proposed by Camanho et al. [9] with the invariant-based approaches to estimate stiffness and strength proposed by Tsai and Melo [10, 11] and with an analytical model based on linear elastic fracture mechanics to estimate the laminate toughness proposed by Camanho et al. [12].

The coupled Finite Fracture Mechanics (FFMs) model proposed by Camanho et al. [9] is used to predict the notched strength of open-hole laminate specimens (Fig 1) with fibre dominated failure. Both a stress-based and energy-based criteria must be satisfied during crack propagation:

$$\begin{cases} \frac{1}{l} \int_R^{R+l} \sigma_{xx}(0, y) dy = X^L \\ \int_R^{R+l} \mathcal{G}_I(a) da = \int_0^l \mathcal{R}(\Delta a) d\Delta a \end{cases} \quad (1)$$

where  $R$  is the hole radius,  $\sigma_{xx}(0, y)$  is the stress distribution along the ligament section perpendicular to the loading direction (along the transverse axis),  $X^L$  is the laminate unnotched strength,  $\mathcal{G}_I(a)$  is the mode I energy release rate (ERR) of a laminated plate with a central circular hole of radius  $R$  and two symmetric cracks propagating from the hole edge,  $\mathcal{R}(\Delta a)$  is the  $\mathcal{R}$ -curve of the laminate and  $l$  is the crack extension at failure.

The first equation corresponds to the average-stress criterion while the second represents an energy balance. Therefore, a stress equilibrium between the average stress in the narrowest critical section with the hole and the maximum admissible strength of the laminate, and an equilibrium between the energy released and the maximum admissible fracture energy of the laminate in a finite length must be satisfied during crack propagation. The model only requires two independent laminate properties: the laminate unnotched strength  $X^L$  and the laminate  $\mathcal{R}$ -curve.

The FFMs model is therefore based on properties at laminate level, which need to be determined each time the layup changes. To determine the laminate unnotched strength  $X^L$ , Furtado et al. [8] proposed the

63 use of the invariant-based approach to estimate stiffness and strength proposed by Tsai and Melo [10, 11].  
 64 This approach is based on the Unit Circle failure envelope, which was proposed by Tsai and Melo [11] as a  
 65 conservative simplification of the last ply failure Omni Strain Failure Envelope. The Unit Circle envelope is  
 66 defined by the uniaxial tensile and compressive strains-to-failure. Following Tsai and Melo [11], the laminate  
 67 unnotched strength under uniaxial loading is estimated by a simple maximum strain criterion:

$$X^L \approx \frac{X}{E_1} \times E^L \quad (2)$$

where  $X$  is the laminate unnotched strength,  $E_1$  is the longitudinal Young's modulus and  $E^L$  is the laminate longitudinal Young's modulus, which can be estimated using the Trace theory and Master Ply concept [10]. Tsai and Melo [10] defined a Master Ply for CFRPs based on the finding that the normalised UD stiffness components of several CFRP systems (normalized by the trace) is almost constant. The authors concluded that the stiffness of CFRPs along the fibre direction is responsible for about 88% of the value of trace, which means that the value of trace can be estimated from the longitudinal stiffness  $E_1$  as

$$Tr \approx \frac{E_1}{0.88} \quad (3)$$

The Young's modulus of a given laminate can be determined as a product of the value of trace and a laminate factor, which can be determined using laminate plate theory and the Master Ply presented in table 1:

$$E^L \approx E_x/Tr \times \frac{E_1}{0.88} \quad (4)$$

**Table 1:** Universal Laminate Factors of the Master Ply.

Lay-up	$E_x/Tr$	$E_y/Tr$	$G_{xy}/Tr$	$\nu_{xy}$
Master Ply	0.880	0.052	0.031	0.320

68 To estimate the laminate  $\mathcal{R}$ -curve, the analytical model proposed by Camanho et al. [12] can be used.  
 69 The model is based on a combination of linear elastic fracture mechanics and laminate plate theory and can  
 70 be used to estimate the fracture toughness of balanced multidirectional laminates,  $G_{Ic}$ , using the fracture  
 71 toughness of the  $0^\circ$  ply,  $G_{Ic}^0$ .

72 Furtado et al. [8] concluded that the framework is able to provide good predictions for the open-  
 73 hole tensile and compressive strengths of general balanced carbon/epoxy laminates with fibre dominated  
 74 failure using only the lay-up, the geometry of the specimen (the radius,  $R$ , and the width,  $W$ ) and three  
 75 ply properties as inputs: the longitudinal Young's modulus,  $E_1$ , the longitudinal strength,  $X$ , and the  
 76 longitudinal crack resistance curve,  $\mathcal{R}$ -curve. Since the model uses only three ply level parameters as  
 77 building blocks, the framework can be particularly useful for preliminary design and optimization, as the

78 number of elementary tests needed to characterize the composite system is drastically reduced. In addition,  
79 due to the computational efficiency of the model it can be used to perform uncertainty quantification and  
80 management (UQ&M) analysis, allowing not only the analysis of the effects of the mean parameters on the  
81 response, but also the analysis of the influence of their variability.

## 82 2.2. Uncertainty quantification of the model parameters

83 The analytical framework [8] summarized in the previous section requires three ply material parameters  
84 to estimate the strength of a multidirectional notched laminate: the longitudinal Young's modulus, the  
85 longitudinal strength and the  $\mathcal{R}$ -curve of the  $0^\circ$  plies. The model was validated using the mean ply properties  
86 determined experimentally, resulting in the prediction of a nominal notched strength for a given nominal  
87 dimension (hole radius and specimen width). In this work, the variability associated with the determination  
88 of the ply properties and the geometry of the specimens is accounted for. The variability associated with the  
89 geometrical parameters (notch radius and specimen width) is directly related to the manufacturing process,  
90 namely the cutting methodology and respective tolerances. Since direct measurements were not available,  
91 the dimensions of the specimen were assumed to follow a uniform distribution.

92 Accounting for the variability of the longitudinal Young's modulus and the longitudinal strength is  
93 straightforward since these properties are obtained directly from the experimental tests and have an asso-  
94 ciated standard deviation. It is assumed here that these two properties follow a normal distribution with  
95 known mean and standard deviation, corresponding to the values obtained experimentally.

96 Accounting for the variability of the  $\mathcal{R}$ -curve is less clear since the  $\mathcal{R}$ -curves are generally not measured  
97 directly but determined from notched strengths measured experimentally. Thus, it is of key importance  
98 to define a methodology to randomly generate statistically representative  $\mathcal{R}$ -curves. Such methodology is  
99 proposed in section 2.2.1.

### 100 2.2.1. Mode I crack resistance curve in the fibre direction

Catalanotti et al. [13, 14] proposed a methodology to determine the  $\mathcal{R}$ -curve of polymer composites reinforced by unidirectional fibres based on the size effect law, i.e the relation between the size of the specimens and their notched strength  $\bar{\sigma}^\infty(w)$ . The size effect law can be determined by experimentally testing geometrically similar double edge notch specimens, i.e. with the same width-to-crack length ratio  $2w/a$  and different widths  $2w$ . The size effect law can be determined by finding a fitting regression that best approximates the experimental data [15] and the  $\mathcal{R}$ -curve parameters (length of the fracture process zone,  $l_{fpz}$ , and the fracture toughness at propagation  $\mathcal{R}_{ss}$ ) can then be obtained as a function of these fitting parameters [15, 13, 14]. Catalanotti et al. [13] also suggested to express the  $\mathcal{R}$ -curve analytically. In this

work, the following analytical expression is proposed to represent the  $\mathcal{R}$ -curve:

$$\begin{cases} R(\Delta a) = R_{ss} [1 - (1 - \Delta a/l_{fpz})^\beta] & \text{if } \Delta a < l_{fpz} \\ R(\Delta a) = R_{ss} & \text{if } \Delta a \geq l_{fpz} \end{cases} \quad (5)$$

101 where  $\beta$  is a parameter determined to obtain the best fit of the  $\mathcal{R}$ -curve. The proposed equation guarantees  
102 that the steady state value of the fracture toughness is reached when  $\Delta a = l_{fpz}$ . Since the mean  $\mathcal{R}$ -curve  
103 is determined from the mean experimental notched strengths of the double edge notch specimens, account-  
104 ing for the variability of the  $\mathcal{R}$ -curves implies accounting for the variability of the size effect law. Two  
105 methodologies to determine the variability of the  $\mathcal{R}$ -curves are proposed in this section.

106 *Method 1.* The variability is obtained by generating a large number of  $\mathcal{R}$ -curves accounting for the variability  
107 of the notched strength ( $\bar{\sigma}^\infty$ ) of the specimens with different geometries by:

- 108 1. Randomly generating  $N_i$  strengths per each specimen geometry following a statistical distribution  
109 determined experimentally for each specimen geometry.
- 110 2. Fitting the data to one of the fitting regressions proposed in Ref. [15].
- 111 3. Determining the  $\mathcal{R}$ -curve parameters ( $l_{fpz}$  and  $\mathcal{R}_{ss}$ ) as proposed in Ref. [15, 13, 14].
- 112 4. Fitting the  $\mathcal{R}$ -curve to the analytical expression proposed in Equation (5) .
- 113 5. Repeat 1-4,  $N$  times obtaining a large number of  $\mathcal{R}$ -curves and the distribution of the fitting parameters.

114 Using this methodology, a set of statistically representative crack resistance curves is obtained. With the  
115 generated  $\mathcal{R}$ -curves it is possible to determine the mean values and standard deviation of the three  $\mathcal{R}$ -curve  
116 fitting parameters ( $l_{fpz}$ ,  $\mathcal{R}_{ss}$  and  $\beta$ ). However, due to the nature of the crack resistance curves, the fitting  
117 parameters cannot be treated independently as that would lead to unrealistic and potentially non-continuous  
118  $\mathcal{R}$ -curves. For this reason, a relation between the parameters should be established as a function of  $\mathcal{R}_{ss}$ , i.e  
119  $l_{fpz} = f(\mathcal{R}_{ss})$  and  $\beta = g(\mathcal{R}_{ss})$ . These functions can vary and should be analysed for each material system  
120 considered. A more detailed analysis is given in section 3.3.

121 *Method 2.* The variability is obtained from the determination of the 95% prediction bounds of the linear  
122 regression used to fit the size effect law measured experimentally. Either the whole set of experimental  
123 points or the mean strengths per specimen geometry can be used, however, the confidence intervals will be  
124 generally narrower if only the mean size effect law is used. This process allows the determination of the  
125 mean  $\mathcal{R}$ -curve and the two 95% confidence  $\mathcal{R}$ -curves. The three  $\mathcal{R}$ -curve parameters and the respective  
126 standard deviations can also be determined.

127 This method provides only three sets of  $\mathcal{R}$ -curve parameters and therefore,  $\mathcal{R}_{ss}$ ,  $l_{fpz}$  and  $\beta$  are considered  
128 independent. This second method is simpler to apply and less computationally expensive, however, the  
129 relation between  $\mathcal{R}_{ss}$  and the remaining parameters has to be assumed, so caution is required when applying  
130 this method.

131 *2.3. Estimation of the B-basis value*

132 In the design of a composite structure it is important to take into account the variability of the design  
133 parameters, namely the material properties. According to the Composite Materials Handbook (CMH17) [1],  
134 variability should be taken into account in the design of composite structures by using the B-basis for the  
135 design allowables. The B-basis (B-value) is a statistically-based design allowable defined as the 95% lower  
136 confidence bound on the tenth percentile of a specified population of measurements [1].

137 By taking the variability of the input parameters (material and geometrical) and using the proposed  
138 analytical model, it is possible to propagate the uncertainty of the input parameters to the notched strength,  
139 i.e. a statistical distribution of the notched strength can be obtained, based on the variability of the input  
140 parameters, which can then be used to compute the statistical design allowables. To obtain the B-value for  
141 the open hole strength, two methodologies have been used: (i) the CMH-17 approach and (ii) a Monte Carlo  
142 based approach.

143 Both approaches rely on the set of material and geometrical properties and respective statistical distri-  
144 bution and differ in how the strength data is dealt with to determine the B-value. Nevertheless, for a given  
145 run of the analytical model the geometrical and material properties are considered deterministic.

146 *CMH-17 approach.* The CMH-17 [1] defines different methods to determine the B-value depending on the  
147 distribution that best fits the data. As summarised in Figure 2, for unstructured data, the CMH-17 suggests  
148 to successively test if the Weibull, normal and lognormal distributions are adequate fits to the data. If any  
149 of these distributions fits the data then the respective methods to calculate the B-basis should be used. If  
150 none of these three distributions can be assumed, nonparametric procedures should be used to determine  
151 the B-value.

152 To find the best fitting distribution, the CMH-17 suggests the use of the Anderson-Darling test. This  
153 test compares the Cumulative Distribution Function (CDF) of the distribution of interest with the CDF of  
154 the data, which allows the determination of a Observance Significance Level (OSL). If the calculated OSL  
155 is greater than 0.05, it is concluded that the distribution analysed fits the data. Otherwise, the analysed  
156 distribution does not fit the data and the subsequent distribution is analysed. Once a fitting distribution has  
157 been found, the B-value can be computed according to the procedures in the CMH-17 for that statistical  
158 distribution [1]. If none of these distributions fit the data, nonparametric procedures are used. These  
159 procedures depend on the sample size, being the Hanson-Koopmans method used for small sample sizes  
160 ( $n < 28$ ). For large sample sizes the B-value can be computed from tabulated data in the CMH-17. For  
161 more information on these procedures, the reader is referred to the CMH-17 [1].

162 *Monte Carlo simulations .* The Monte Carlo Methods (MCS) rely on the repeated random sampling to  
163 obtain numerical results. To determine the B-value using this approach it is necessary to run the analytical



164 model a large number of times to determine an Empirical Cumulative Distribution Function (ECDF) for  
 165 the parameter in study, namely the notched strength. For each set of  $n$  results, where  $n$  is the sample size  
 166 that should be large enough to be representative of the population, it is possible to determine the ECDF  
 167 and extract the 10th percentile value,  $P_{10,j}$ . This process is repeated  $N$  times, determining a distribution  
 168 for the 10th percentile. From this distribution the B-value can be computed by considering the 95% lower  
 169 confidence bound [16], which corresponds to the 5<sup>th</sup> percentile of the ECDF. The MCS based methodology  
 170 to calculate the B-value can be summarised as follows (see Figure 3):

- 171 1. Design of the experiments (DOE). The material properties and geometrical parameters are distributed  
 172 according to their associated statistical distributions to define the uncertainty quantification and man-  
 173 agement matrix. Using the current analytical framework, the dimensions of the matrix are  $n \times 5$  where  
 174  $n$  are the different cases to be analysed and 5 are the model input parameters ( $E_{11}$ ,  $X_T$ ,  $R_{ssT}$ ,  $R$  and  
 175  $W$ ).
- 176 2. Notched strength computation. For each case  $i$  the notched strength ( $\bar{\sigma}_i^\infty$ ) is calculated using the  
 177 analytical model described in Section 2.1.
- 178 3. Determination of the 10th percentile. Once all the cases have been computed ( $\bar{\sigma}_{i:1 \rightarrow n}^\infty$ ) the ECDF of  
 179 the notched strengths is used to determine the  $P_{10,j}$ .
- 180 4. Computation of the B-basis allowable. Steps 1, 2 and 3 are repeated  $N$  times to obtain the ECDF of  
 181 the  $P_{10,j:1 \rightarrow N}$  and to determine the 5<sup>th</sup> percentile which corresponds to the B-basis value.

182 If the sample size ( $n$ ) is large enough, then the 10<sup>th</sup> percentile of the population can be directly approx-  
 183 imated by the 10<sup>th</sup> percentile of the sample, as the variability between the samples will be minimal. This  
 184 will be explored in more detail in Section 5.1.

### 185 3. Case study

#### 186 3.1. Description of the case

187 To exemplify and validate the methodology proposed to calculate the B-value of the notched strength,  
 188 IM7/8552 [90/0/-45/45]<sub>3s</sub> quasi isotropic laminate with a central circular hole loaded in tension was used.  
 189 Hole diameter-to-width ratios of  $0.05 < 2R/W < 0.6$  and hole diameters of 2, 4, 6, 8 and 10mm were used.

190 As explained in section 2.2, the variability associated with the material parameters and with the geometry  
 191 of the specimens is considered to calculate the B-value. The input parameters used are presented hereafter.

#### 192 3.2. Uncertainty quantification associated with the geometry of the specimens

193 The variability associated with the geometry of the specimens is directly related to the manufacturing  
 194 process, namely the cutting methodology and respective allowed tolerances. The specimen dimensions were

195 assumed to follow a uniform distribution with a maximum deviation of  $\pm 2\%$  of the nominal value of the  
 196 width and hole diameter.

**Table 2:** Variability of the geometry of the specimen [17].

Geometry	$W$ [mm]	$R$ [mm]
<i>tol</i>	$\pm 2\% \times W$	$\pm 2\% \times R$

### 197 3.3. Uncertainty quantification associated with the determination of the material properties

198 In this work, it is assumed that the material properties follow a normal distribution with known mean  
 199 and standard deviation. These properties are summarised in Table 3. The uncertainty related to the  
 200 longitudinal Young's modulus and strength is directly related to the the mean values ( $\bar{x}$ ) and respective  
 201 standard deviation ( $s$ ) determined experimentally [18] while the variability of the  $\mathcal{R}$ -curve is determined as  
 202 explained in section 2.2.

**Table 3:** Value of the material properties used for the analysis [18].

IM7/8552	$E_1$ [GPa]	$X_T$ [GPa]	$\mathcal{R}_{ssT}$ [N/mm]
$\bar{x}$	171.42	2323.47	206.75
$s$	2.38	127.45	23.64

203 The determination of the  $\mathcal{R}$ -curve is based on the size effect law which can be determined from the  
 204 strengths of geometrically similar double edge notched specimens with different widths. Table 4 shows the  
 205 notched strengths and respective standard deviations of the double edge notch tension specimens that were  
 206 used to determine the longitudinal crack resistance curve of IM7/8552 material system [13].

**Table 4:** Double Edge Notched Tension Strength for IM7/8552 [90/0]<sub>8s</sub> [13].

Ref.	$w$ [mm]	$\bar{x}$ [MPa]	$s$ [MPa]
B	7.5	309	9
C	10	289	16
D	12.5	269	11
E	15	256	10

207 Using Method 1 described in Section 2.2.1, a set of statistically representative crack resistance curves,  
 208 with a known mean and standard deviation of the three fitting parameters ( $l_{fpz}$ ,  $\mathcal{R}_{ss}$  and  $\beta$ ) is obtained, as

209 shown in Figure 4.

210 As explained in section Section 2.2.1, the fitting parameters of the crack resistance curves cannot be  
 211 treated independently as that would potentially lead to non admissible  $\mathcal{R}$ -curves. For this reason, a depen-  
 212 dence between the parameters was established as a function of  $\mathcal{R}_{ss}$ . As shown in figure 5, it was found that  
 213  $l_{fpz}$  varies linearly with  $\mathcal{R}_{ss}$  and  $\beta$  is almost constant for the case analysed. Therefore, the crack resistance  
 214 curves can be defined as a function of  $\mathcal{R}_{ss}$ .  $\mathcal{R}_{ss}$  is generated randomly following a normal distribution  
 215 with a know mean (206.75 N/mm) and standard deviation (23.64 N/mm) and the other two parameters are  
 216 estimated as:

$$l_{fpz} = 2.7776 \times 10^{-2} \times \mathcal{R}_{ss} - 3.0598 \quad [\text{mm}]$$

$$\beta = 2.9027 \quad [-]$$

217 Using Method 2 the variability is obtained from the determination of the 95% prediction bounds of the  
 218 fitting of the size effect law. Either the whole set of experimental points or the mean strengths per specimen  
 219 geometry can be used. In this study only the mean strengths were used since the full set of results was not  
 220 available.

221 Since this method provides only three sets of  $\mathcal{R}$ -curve parameters, the relation between  $l_{fpz}$ ,  $\mathcal{R}_{ss}$  and  $\beta$   
 222 is undefined. However, using method 1, it was shown that a linear functions can be used to relate  $\mathcal{R}_{ss}$  to  $l_{fpz}$   
 223 and  $\beta$ , and so the fitting parameters of the curves can be easily determined as a function of  $\mathcal{R}_{ss}$  as shown in  
 224 figure 5. Using this method,  $\mathcal{R}_{ss}$  is generated randomly following a normal distribution with a know mean  
 225 (205.26 N/mm) and standard deviation ( 14.83 N/mm) and the other two parameters are estimated as:

$$l_{fpz} = 2.8654 \times 10^{-2} \times \mathcal{R}_{ss} - 3.2701 \quad [\text{mm}]$$

$$\beta = 2.9024 \quad [-]$$

226 As shown in figure 5 the fitting curves obtained with both methods show similar trends. Figure 6 shows  
 227 the normal distribution and the corresponding average and 95% IC  $\mathcal{R}$ -curves obtained with both methods.  
 228 Only a 1.5 N/mm difference in the mean  $\mathcal{R}_{ss}$  using methods 1 and 2 was found. However, since the standard  
 229 deviation obtained using method 2 is around 40% lower than the one measured using method 1 because the  
 230 confidence bounds were determined using the mean double edge notch strengths, the normal distribution  
 231 of  $\mathcal{R}_{ss}$  is significantly narrower if method 2 is used. Using the whole set of data would be preferred in  
 232 method 2. Therefore, in, method 1 was used to characterize the distribution of the crack resistance curve  
 233 parameters.

#### 234 4. Sensitivity analysis

235 Due to the analytical nature of the model, it is possible to run a large number of simulations within  
 236 a reasonable time frame, enabling the performance of numerical analysis that would not be possible via  
 237 experimental characterization or finite element simulations.

238 The proposed framework depends on three material properties and two geometrical properties. It is  
 239 interesting to understand their influence on the expected notched strength of the laminate selected for this  
 240 study. To do so, a sensitivity analysis was performed on these five parameters. The sensitivity analysis is  
 241 performed by considering that the parameter in study varies while the remaining are kept constant and with  
 242 a value equal to the nominal one. Here the material and layup considered are the ones presented in Section  
 243 3 and an open-hole tension specimen with width equal to 36 mm and hole radius of 3 mm is considered. For  
 244 each material property a range from  $\bar{x}_i - 3s_i$  to  $\bar{x}_i + 3s_i$  was considered. For the geometrical parameters a  
 245 variation of  $\pm 2\%$  was considered. The results of the sensitivity analysis are shown in Figure 7.

246 From the sensitivity analysis, it is possible to conclude that, as expected, the material properties have  
 247 a larger influence on the notched strength than the geometrical properties. For the Young's modulus the  
 248 variation of the OH strength is linear, being lower for lower elastic moduli. Both the tensile strength and  
 249 toughness of the material have a more complex influence on the open hole strength of the material. In  
 250 addition, both have a higher influence on the open hole strength of the material, therefore, it is essential to  
 251 accurately characterize these properties to ensure accurate predictions of the notched strength of composite  
 252 laminates.

#### 253 5. UQ&M framework validation

254 In this section the sample sizes required to accurately take into account geometrical and material vari-  
 255 ability within the UQ&M framework is analysed and the results are validated against available experimental  
 256 data.

##### 257 5.1. Effect of the sample size on the mean notched strength and on B-basis value using the MCS method

258 To validate the proposed UQ&M methodology, it is important to analyse the number of simulations  
 259 required to ensure an accurate determination of the output parameters. The fact that the framework used is  
 260 fully analytical, allows a very large number of simulations to be performed, however, it is of key importance  
 261 to ensure that the open-hole strength (mean and B-basis) are determined efficiently, i.e. performing the  
 262 minimum number of simulations required to obtain accurate and statistically consistent results.

263 The methodology to determine the B-basis using MCS is described in Section 2.3. This methodology  
 264 requires the computation of  $n \times N$  number of simulations to determine the B-value. This may lead to a  
 265 very high number of simulations, rendering the methodology computationally expensive. However, it is

possible to determine the B-basis based on a smaller number of simulations if we consider  $N = 1$  and have a sample size ( $n$ ) sufficiently large to be representative of the population of results. With this methodology, the B-basis can be approximated by the 10<sup>th</sup> percentile of the sample, therefore, reducing the number of simulations to be performed.

To determine the minimum sample size that ensures this representativeness, the sample size was varied between 10 and 100,000. For each sample size 10 random samples were obtained to compute both the average and standard deviation of the mean open hole strength ( $\bar{\sigma}^\infty$ ) and the respective B-basis ( $P_{10}$ ). Figure 8 shows the convergence analysis of both the average OH strength and B-basis.

**Table 5:** Mean value and variance of the average OH strength ( $\bar{\sigma}^\infty$ ) and B-value ( $P_{10}$ ) according to the number of samples when  $N = 10$ .

Samples, $n$	$\bar{\sigma}^\infty$		$P_{10}$	
	$\bar{\sigma}^\infty$ [MPa]	$s_{\sigma^\infty}$ [MPa]	$P_{10}$ [MPa]	$s_{P_{10}}$ [MPa]
10	450.77	3.11	436.83	6.15
50	452.61	0.62	440.15	2.90
100	452.54	0.91	441.33	2.52
1000	452.68	0.24	441.86	0.53
10000	452.63	0.11	441.65	0.21
30000	452.62	0.04	441.64	0.13
100000	452.62	0.03	441.64	0.05

Analysing the data, it is possible to conclude that the variability of both the mean OH strength and B-basis is reduced with increasing sample size, however, the computational cost increases. It is possible to conclude that for a sample size of 10,000 the Coefficient of Variation (CoV) of both the mean OH strength and B-basis is very low, 0.02% and 0.05%, respectively. Therefore, a sample size of 10,000 can be considered as representative of the population of results and be used to obtain the average OH strength and respective B-basis. If we consider a sample size of 30,000, which has a three times increase in computational time, there is an insignificant reduction in the CoV for the mean strength and B-basis (to 0.01% and 0.03% respectively). Therefore, it is concluded that a sample size of 10,000 is large enough and ensures a good compromise between the accuracy and computational cost.

To summarize, the calculation of the B-basis allowable using MCS can be done in a computationally efficient way by running 10,000 simulations ( $N = 1$ ) and determining the 10<sup>th</sup> percentile of the sample as this number of samples is considered representative of the whole population. This methodology will be considered for the determination of the B-basis allowables using Monte Carlo simulations in the following sections.

### 288 5.2. Effect of the sample size on the B-basis using the CMH-17 approach

289 In Section 2.3 the methodology to determine the B-basis allowable based on the CMH-17 was presented.  
290 In this section a comparison between the B-basis determined using this methodology is compared with the  
291 results obtained using Monte Carlo simulations. The CMH-17 approach is useful since it takes into account  
292 the size of the population and the distribution that most accurately represents the data to determine the  
293 B-basis and therefore, a good estimate of this parameter can be obtained using a small number of data  
294 points.

295 In Figure 9 the B-basis allowable for OH strength determined using the CMH-17 methodology for different  
296 sample sizes is shown and is compared with the value obtained using MCS. For each sample size, 100  
297 simulations were performed based on different randomly generated samples, to get not only an average value  
298 for the B-basis but also to determine its dispersion for each sample size.

299 As the sample size increases, the B-value determined with the CMH-17 approach becomes less conser-  
300 vative and the confidence interval is reduced, as bigger samples are considered more representative of the  
301 population. In Table 6 the results of the B-value are also shown for different sample sizes. In addition,  
302 the methodologies from the CMH-17 that were applied for each sample are shown, as different distributions  
303 were seen to best fit the data depending on the sample considered.

304 For a sample size of 30 it is seen that the variability of the calculated B-basis increases. This increase  
305 in variability with increased sample size can be justified with the fact that for the mentioned sample size,  
306 there was an increase in the number of samples that could not be represented by a Weibull distribution (see  
307 Table 6) and, therefore, a different distribution had to be used, or even the non-parametric methodology,  
308 which increased the dispersion in the determination of the B-basis.

309 In the remainder of this study, a sample size of 25 is considered when determining the B-basis with the  
310 CMH-17 methodology, as it is seen to be a reasonable sample size, which might be used in experimental  
311 campaigns, that ensures a good B-basis estimation.

### 312 5.3. Validation of the UQ&M framework

313 A comparison between the experimental results presented in Ref. [18] and the predictions using the  
314 proposed framework is shown in Figure 10. Both the OH strengths computed using the nominal values  
315 of the material and geometrical properties and the results obtained when these properties are considered  
316 stochastic are included. The latter methodology allows not only to obtain the average value for OH strength  
317 for each geometry but also the expected variability.

318 As expected, using the nominal values of the geometrical and material parameters results in approxi-  
319 mately the same open hole strength as the average of the stochastic results, ensuring the consistency of the  
320 uncertainty quantification framework developed. The results shown in Figure 10 indicate that the proposed

**Table 6:** Results for the B-basis determination using the CMH-17 methodology.

Samples, $n$	Weibull	Normal	Lognormal	Non parametric	$\bar{B}$ [MPa]	$s_B$ [MPa]	$IC_B$ [ $\pm$ MPa]	error %
5	92	8	0	0	411.35	17.992	3.5696	6.858
10	93	3	0	0	428.77	9.5808	1.9008	2.9152
15	88	3	0	0	431.84	8.0774	1.6026	2.2193
20	94	2	0	0	434.78	4.2685	0.84686	1.553
25	94	2	0	0	435.92	4.3825	0.86948	1.2953
30	91	4	0	5	438.17	7.051	1.3989	0.78675
40	94	3	0	3	437.74	3.4001	0.67458	0.88285
50	92	5	0	3	437.24	3.2488	0.64456	0.99621
100	78	5	0	17	438.76	2.7482	0.54525	0.65224
150	91	1	0	8	439.43	1.5205	0.30167	0.50112

framework is capable of accurate predictions of the open-hole tension strength. The maximum error obtained for this case study was 12% which, taking into account that this is an analytical formulation with very reduced computational cost, is very reasonable.

As the developed framework is aimed at the determination of the B-basis allowable for open hole strength, the comparison between the B-basis obtained analytically, with the two presented methods, and experimentally is shown in Figure 11. For consistency, as the experimental sample size used was 5 specimens [18], the same sample size was considered when computing the B-value with the CMH-17 approach. This allows a direct comparison between the experimental B-basis and the one obtained numerically. Nevertheless, the results with a sample size of 25 are also shown. To ensure that the results obtained did not result in outliers, 10 B-basis calculations were performed for each geometry. For the Monte Carlo simulations approach a larger number of simulations is always required to ensure the representativeness of the population, therefore, the sample size was kept at 10,000.

Observing the previous results it is concluded that the B-value determined with the CMH-17 approach is similar to that obtained experimentally, for the same sample size ( $n = 5$ ), which reflects not only the ability of the framework to accurately compute the open hole strength of a given configuration, but also its ability to propagate the uncertainty of the input parameters to the open hole strength. The B-basis obtained with the MCS approach is always less conservative than the one obtained with the CMH-17 approach due to the larger sample size, which is reflected in the results of Figure 11 and was also obtained in the numerical comparison provided in Figure 9. The same sample size effect can be observed comparing the CMH-17 approach with  $n = 5$  and  $n = 25$ . Nevertheless, the results obtained are consistent with the experimental

341 ones.

## 342 6. Applications

### 343 6.1. Design charts for open hole tension

344 Taking into account that the analytical UQ&M framework developed enables the quick estimation of the  
345 notched strength of laminated composites and the respective B-basis allowables, it can be used to generate  
346 design charts and compare the performance of different layups and materials in a preliminary stage of the  
347 design process.

348 Following Camanho et al. [9], design charts that relate the diameter-to-width ratio to the notched  
349 tensile strength of specimens with diameters 2, 6 and 10mm were generated. Monte Carlo simulations with  
350  $n = 10,000$  were used to generate the average notched strength distribution of each point and compute the  
351 mean value and respective B-basis allowable, as defined in Section 5.1 (Fig. 12). To calculate the B-value,  
352 the CMH-17 approach could also have been used without significant loss of accuracy as shown in Fig. 13 for  
353 a specimen with a hole radius of 6mm, however, given the computational efficiency of the model, performing  
354 Monte Carlo simulations is not a particularly limiting approach.

355 Experimentally generating statistically representative design charts is unreasonable given the number of  
356 specimens, specimen configurations, layups and materials required to populate them. The analytical UQ&M  
357 framework here proposed can help overcome this limitation and assist engineers during the design process  
358 given its simplicity and efficiency.

### 359 6.2. Influence of the load direction on the open hole strength

360 The framework was developed to work as a fast design tool that is capable to predict the notched strength  
361 of a laminate in the most varied cases. In this section, the variation of the loading direction and its effect on  
362 the open hole tensile strength is explored. The design of a laminate for a given structure is usually optimized  
363 for a given load direction, however, it is not acceptable to have a laminate whose strength is very high in  
364 one direction but any misalignment in the load, which most certainty occurs in real usage, leads to a high  
365 reduction of its strength. Therefore, being able to rapidly predict the notched strength in a multitude of  
366 loading directions is an useful design tool. The variation of the mean open hole strength as a function of  
367 the load direction and the respective 95% confidence interval and predicted B-basis value based on MCS  
368 ( $n = 10,000$ ) and on the CMH-17 ( $n = 25$ ) are shown in Figure 14. This analysis was done for the baseline  
369 configuration of a width of 36 mm and a radius of 6 mm.

370 Due to the fact that the laminate in study is quasi isotropic (Section 3), the notched strengths at 0, 45  
371 and 90° are equal. However the strength is reduced for any other load direction. From the shown results  
372 it is possible to conclude that with the given laminate the reduction of strength due to changing the load



373 direction is small, being the lowest value equal to 377.1 MPa, while the maximum (for 0, 45 and 90°) is  
374 equal to 455.0 MPa. Additionally, it is observed that small variations around the principal load direction  
375 (0°) have only a small effect on the notched strength. Regarding the B-basis allowable it is seen that for the  
376 analysed cases the results from the CMH-17 and MCS approach are similar. It is interesting to note that  
377 the difference between the B-basis and the mean value for the open hole strength is not constant throughout  
378 the angle space. This difference is highest when the average strength is lowest, which creates a wider span  
379 of the B-basis allowable between its maximum and minimum. This can be explained by the fact that at  
380 these load angles the variability of the material and geometrical parameters leads to a higher variability of  
381 the notched strength and, therefore, a reduced B-basis allowable.

### 382 6.3. Large damage capability

383 The proposed framework was developed with the aim of predicting the open-hole strength of laminate  
384 structures, however, it is general enough to be able to predict the strength of different notched geome-  
385 tries, provided the stress distribution and energy release rate are known for those geometries and loading  
386 conditions. As it is well known, the tensile strength of composite laminates in the presence of through-the-  
387 thickness notches is significantly affected by size, being the smallest geometries strength-dominated and large  
388 ones toughness-dominated [19]. Therefore, the analysis tools must be able to account this distinct material  
389 behaviours when computing the notched strength. Following Arteiro et al. [19] the developed framework  
390 is used to predict the large damage capability of the laminate in study, considering a centre notched plate  
391 under tension loading (Figure 15).

392 In Figure 16, the mean notched strength and respective B-basis allowable of centre notched plates with  
393 a constant plate width-to-notch length ratio ( $W/2a$ ) equal to 7.5 with different notch sizes are shown. The  
394 notches were considered to have a constant tip radius of 0.5 mm ( $h = 1$  mm). For the smaller geometries the  
395 traditional methods that only consider the steady state value of the fracture toughness in their formulation  
396 are able to predict the notched strength, however, for larger specimens and large damage capability analysis  
397 the introduction of the R-curve in the modelling strategy is of utmost importance [19]. This is taken into  
398 account in the present framework, which increases the reliability of the modelling strategy. It is possible to  
399 see in Figure 16 that both the mean notched strength and its respective B-basis allowable follow the same  
400 trends, being the difference between both parameters similar throughout the analysed space.

401 In this study, two notched geometries are analysed, open-hole tension and centre-notched tension, however  
402 the framework is generic enough to take into account other geometries such as open-hole compression and  
403 bolted joints failing by net-tension [20], given that the stress concentration factors and energy release rates  
404 of the configuration in study are known.

## 405 7. Conclusions

406 The current approach to determine the design allowables in the aeronautical industry relies in extensive  
407 testing based on the building block approach, which makes the selection and certification of composite  
408 materials expensive and time consuming. To increase the efficiency of material and laminate selection  
409 during preliminary design, there is a need to reduce the number of experimental tests required during this  
410 process, and replace or complement them with accurate modelling strategies coupled with the statistical  
411 tools to account for material, manufacturing and geometrical variability.

412 In this work an UQ&M framework was developed to estimate the B-basis design allowable for notched  
413 components. This framework is based on the analytical model developed by Furtado et al. [8] that only  
414 requires three lamina level material properties to estimate the notched strength of a laminate, given that the  
415 stress distribution and energy release rate are known for the geometries and loading conditions in study. This  
416 model is coupled with the statistical tools required to take into account the variability of both the material  
417 and geometrical parameters and propagate this uncertainty to the notched strength, therefore allowing the  
418 quick estimation of B-basis allowable.

419 The developed framework allows the computation of the B-basis allowable based on Monte Carlo simu-  
420 lations and on the the approach proposed in the CMH-17, which requires a lower number of samples. Both  
421 approaches are compared and it is concluded that the CMH-17 gives a more conservative estimation of  
422 the B-basis allowable due to the lower number of samples usually used. Given that the current modelling  
423 strategy is computationally efficient, the usage of Monte Carlo simulations allows the estimation of a less  
424 conservative B-basis as a large number of samples can be computed in a reasonable time frame. This makes  
425 the proposed framework specially interesting in the preliminary design and selection of materials and layouts.

426 The proposed framework is validated successfully with the open-hole tension experimental campaign for  
427 the IM7/8552 material [18], ensuring a maximum error around 10%, which is very reasonable given the  
428 analytical formulation of the model.

429 Additionally, the framework is used to develop design charts for notched specimens, tools that are useful  
430 for design engineers and would otherwise be infeasible to attain as they require a large number of testing or  
431 time consuming simulations to be performed.

432 Note that in this paper, the methodology is applied to open hole tension and center notched specimens,  
433 but the framework can be enriched with other notched configurations, provided the stress distribution and  
434 energy release rate are known for those geometries and loading conditions.

## 435 Acknowledgements

436 OV acknowledges the support of the Catalan Government, under the Grant 2018FLB.00904 CF and  
437 RT acknowledge the support of the Portuguese Governments Fundação para a Ciência e Tecnologia, under

438 the Grants SFRH/BD/115859/2016 and SFRH/BD/115872/2016. AA would like to thank the financial  
439 support provided by FCT – Fundação para a Ciência e a Tecnologia through National Funds in the scope  
440 of project MITP-TB/PFM/0005/2013. PC gratefully acknowledges the funding of Project PTDC/EMS-  
441 PRO/4732/2014, cofinanced by Programa Operacional Competitividade e Internacionalização and Programa  
442 Operacional Regional de Lisboa, through Fundo Europeu de Desenvolvimento Regional (FEDER) and by  
443 National Funds through FCT Fundação para a Ciência e Tecnologia. AT gratefully acknowledges the  
444 funding of the Project TRA2015-71491-R, cofinanced by the Spanish Government (Ministerio de Economía  
445 y Competitividad) and the European Social Fund.

- 446 [1] CMH-17, Composites material handbook 17g. vol. 1 guidelines for characterization of structural materials (2012).  
447 [2] C. Rousseau, How various uncertainties and assumptions affect b-basis allowables development., Lockheed Martin Corpo-  
448 ration, 2013.  
449 [3] P. R. Spendley, Design allowables for composite aerospace structures, Ph.D. thesis, University of Surrey (2012).  
450 [4] F. Abdi, E. Clarkson, C. Godines, S. DorMohammadi, Ab basis allowable test reduction approach and composite generic  
451 basis strength values, in: 18th AIAA Non-Deterministic Approaches Conference, 2016, p. 0951.  
452 [5] Y. Zhang, J. Schutte, J. Meeker, U. Palliyaguru, N. H. Kim, R. T. Haftka, Predicting b-basis allowable at untested  
453 points from experiments and simulations of plates with holes, in: 12th world congress on structural and multidisciplinary  
454 optimization, Braunschweig, Germany. URL: <https://www.researchgate.net/publication/318909364>, 2017.  
455 [6] G. Abumeri, F. Abdi, K. Raju, J. Housner, R. Bohner, A. McCloskey, Cost effective computational approach for generation  
456 of polymeric composite material allowables for reduced testing, in: Advances in Composite Materials-Ecodesign and  
457 Analysis, InTech, 2011.  
458 [7] K. Nam, K. J. Park, S. Shin, S. J. Kim, I.-H. Choi, Estimation of composite laminate design allowables using the statistical  
459 characteristics of lamina level test data, International Journal of Aeronautical and Space Sciences 16 (3) (2015) 360–369.  
460 [8] C. Furtado, A. Arteiro, M. Bessa, B. Wardle, P. P. Camanho, Prediction of size effects in open-hole laminates using only  
461 the Youngs modulus, the strength, and the R-curve of the 0 ply, Composites Part A: Applied Science and Manufacturing  
462 101 (AAA) (2017) 306–317.  
463 [9] P. P. Camanho, G. Erin, G. Catalanotti, S. Mahdi, P. Linde, A finite fracture mechanics model for the prediction of  
464 the open-hole strength of composite laminates, Composites Part A: Applied Science and Manufacturing 43 (8) (2012)  
465 1219–1225.  
466 [10] S. W. Tsai, J. D. D. Melo, An invariant-based theory of composites, Composites Science and Technology 100 (2014)  
467 237–243.  
468 [11] S. W. Tsai, J. D. D. Melo, A unit circle failure criterion for carbon fiber reinforced polymer composites, Composites  
469 Science and Technology 123 (2016) 71–78.  
470 [12] P. P. Camanho, G. Catalanotti, On the relation between the mode I fracture toughness of a composite laminate and that  
471 of a 0 ply: Analytical model and experimental validation, Engineering Fracture Mechanics 78 (13) (2011) 2535–2546.  
472 [13] G. Catalanotti, A. Arteiro, M. Hayati, P. P. Camanho, Determination of the mode I crack resistance curve of polymer  
473 composites using the size-effect law, Engineering Fracture Mechanics 118 (2014) 49–65.  
474 [14] G. Catalanotti, J. Xavier, P. P. Camanho, Measurement of the compressive crack resistance curve of composites using the  
475 size effect law, Composites Part A: Applied Science and Manufacturing 56 (2014) 300–307.  
476 [15] Z. P. Bazant, J. Planas, Fracture and size effect in concrete and other quasibrittle materials, Vol. 16, CRC press, 1997.  
477 [16] S. Chakraborti, J. Li, Confidence interval estimation of a normal percentile, The American Statistician 61 (4) (2007)  
478 331–336.

- 479 [17] W. C. (PA), A. S. for Testing, M. (ASTM), Standard test method for open hole tensile strength of polymer matrix  
480 composite laminates, ASTM D 5766/D 5766M 02a.
- 481 [18] P. P. Camanho, P. Maimí, C. Dávila, Prediction of size effects in notched laminates using continuum damage mechanics,  
482 Composites science and technology 67 (13) (2007) 2715–2727.
- 483 [19] A. Arteiro, G. Catalanotti, J. Xavier, P. Camanho, Large damage capability of non-crimp fabric thin-ply laminates,  
484 Composites Part A: Applied Science and Manufacturing 63 (2014) 110–122.
- 485 [20] G. Catalanotti, P. Camanho, A semi-analytical method to predict net-tension failure of mechanically fastened joints in  
486 composite laminates, Composites Science and Technology 76 (2013) 69–76.

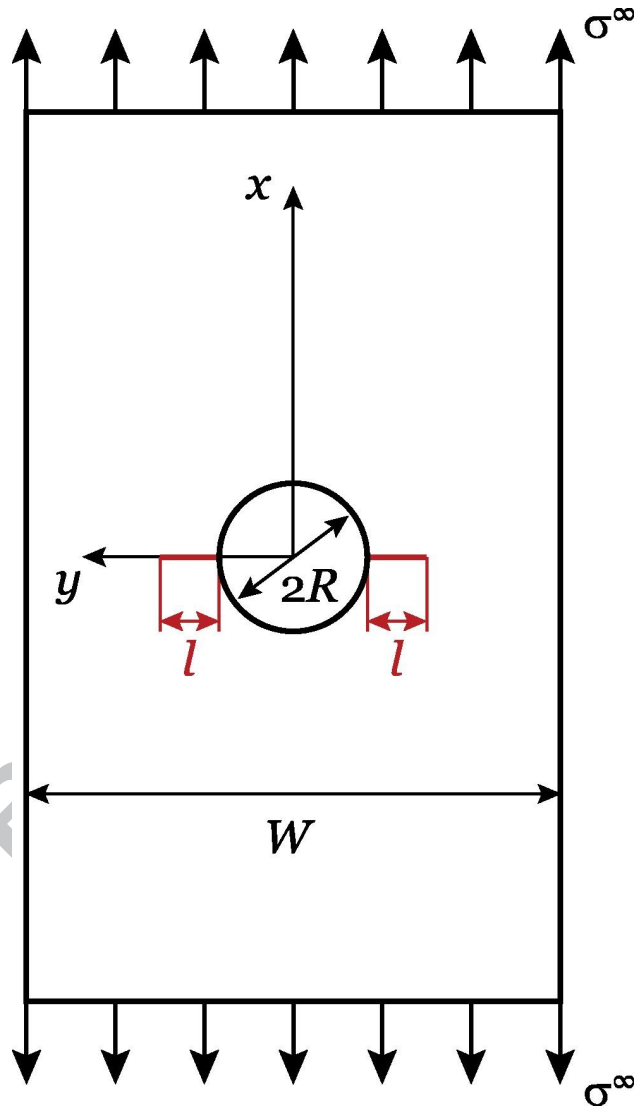
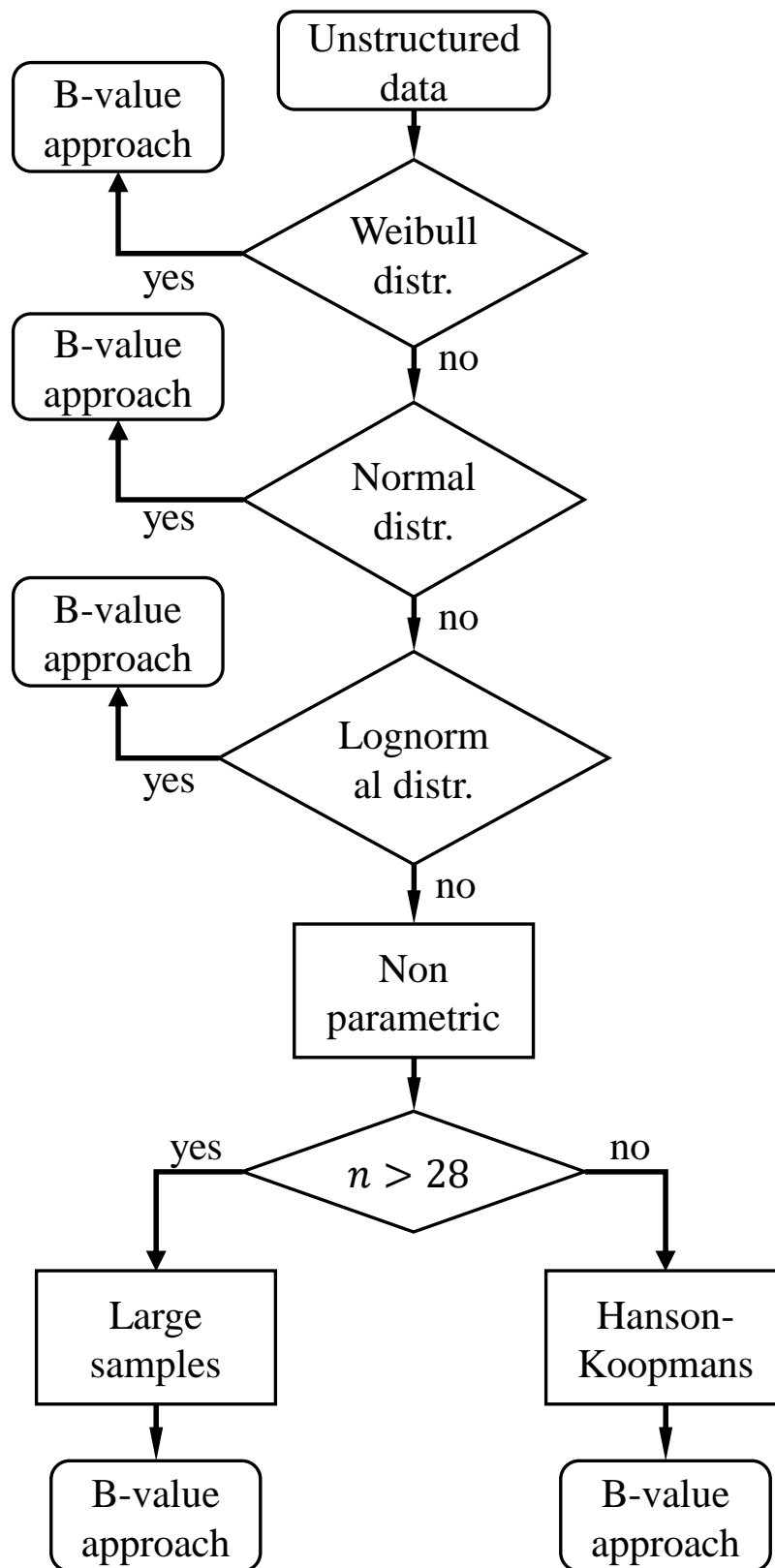
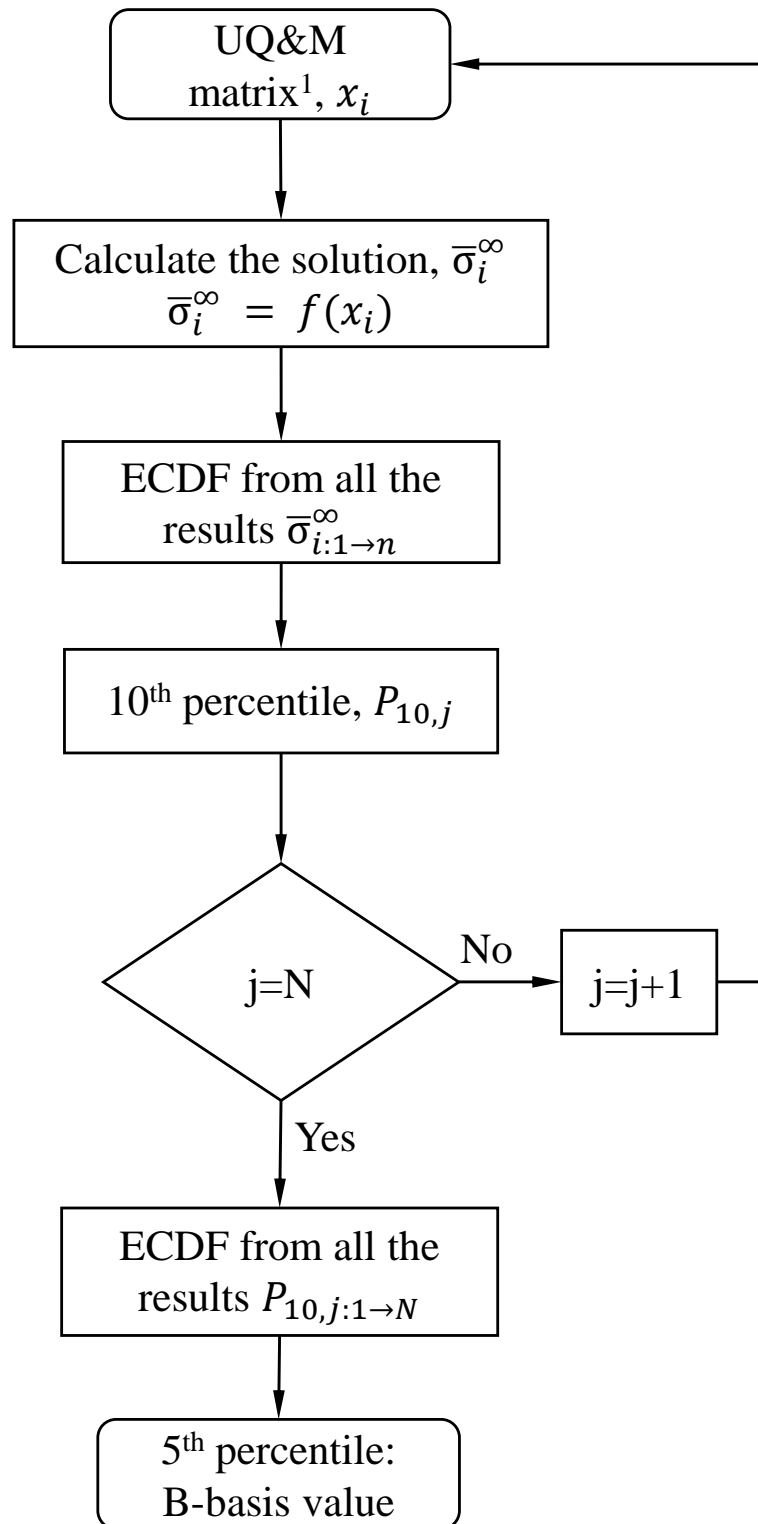


Figure 1: Notched laminate with central circular open hole [8].



**Figure 2:** Schematic representation of the steps to calculate the B-value using the CMH-17 methodology.



<sup>1</sup> UQ&M matrix dimensions are:  $n$  different cases per 5 input variables ( $x_i$ ); in the first iteration  $j = 1$ .

**Figure 3:** Schematic representation of the steps to calculate the B-value using the Monte Carlo based methodology.

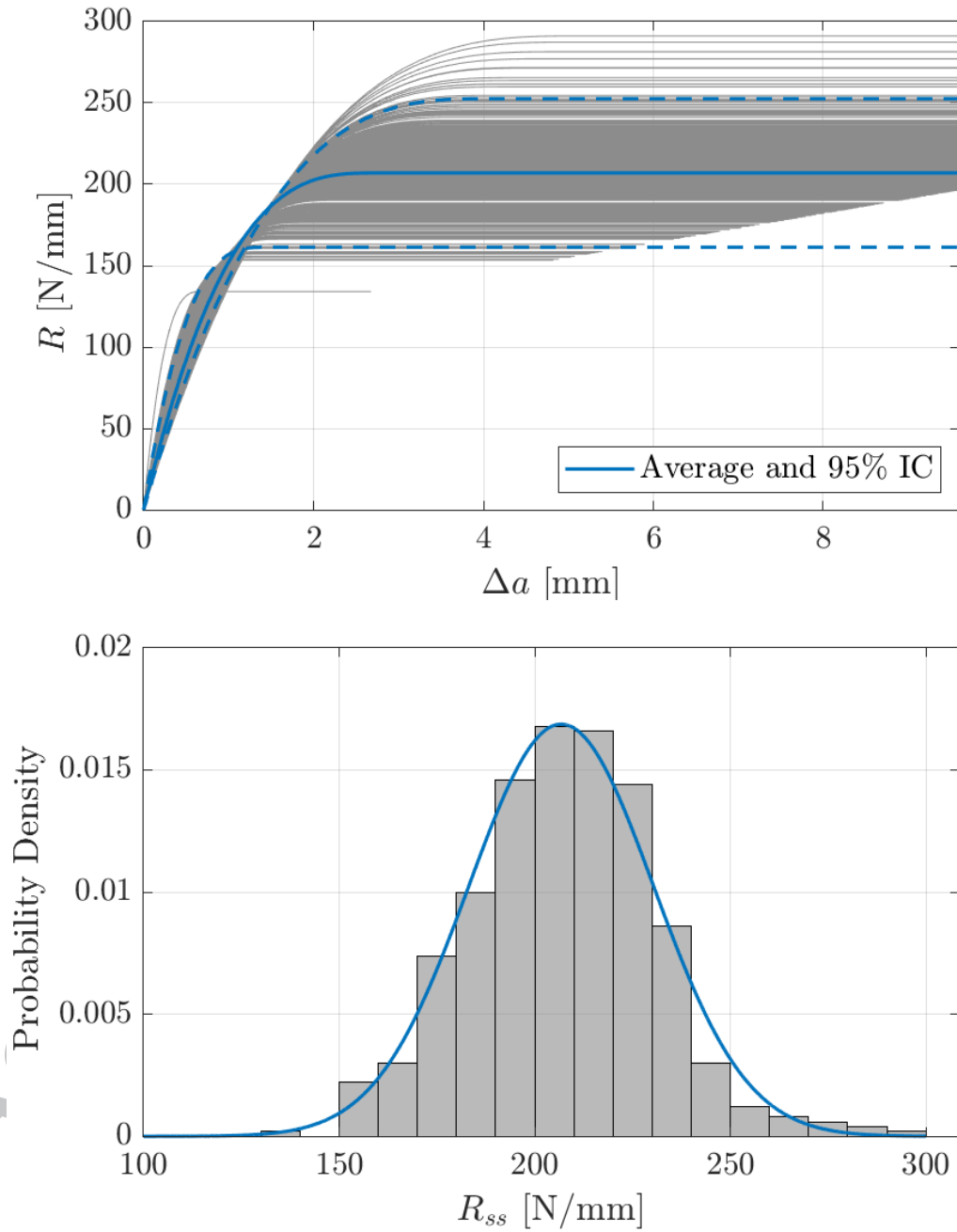


**Figure 4:** Schematic representation of randomly generated  $\mathcal{R}$ -curves using method 1 (top) and distribution of the steady state fracture toughness  $R_{ss}$  (bottom).



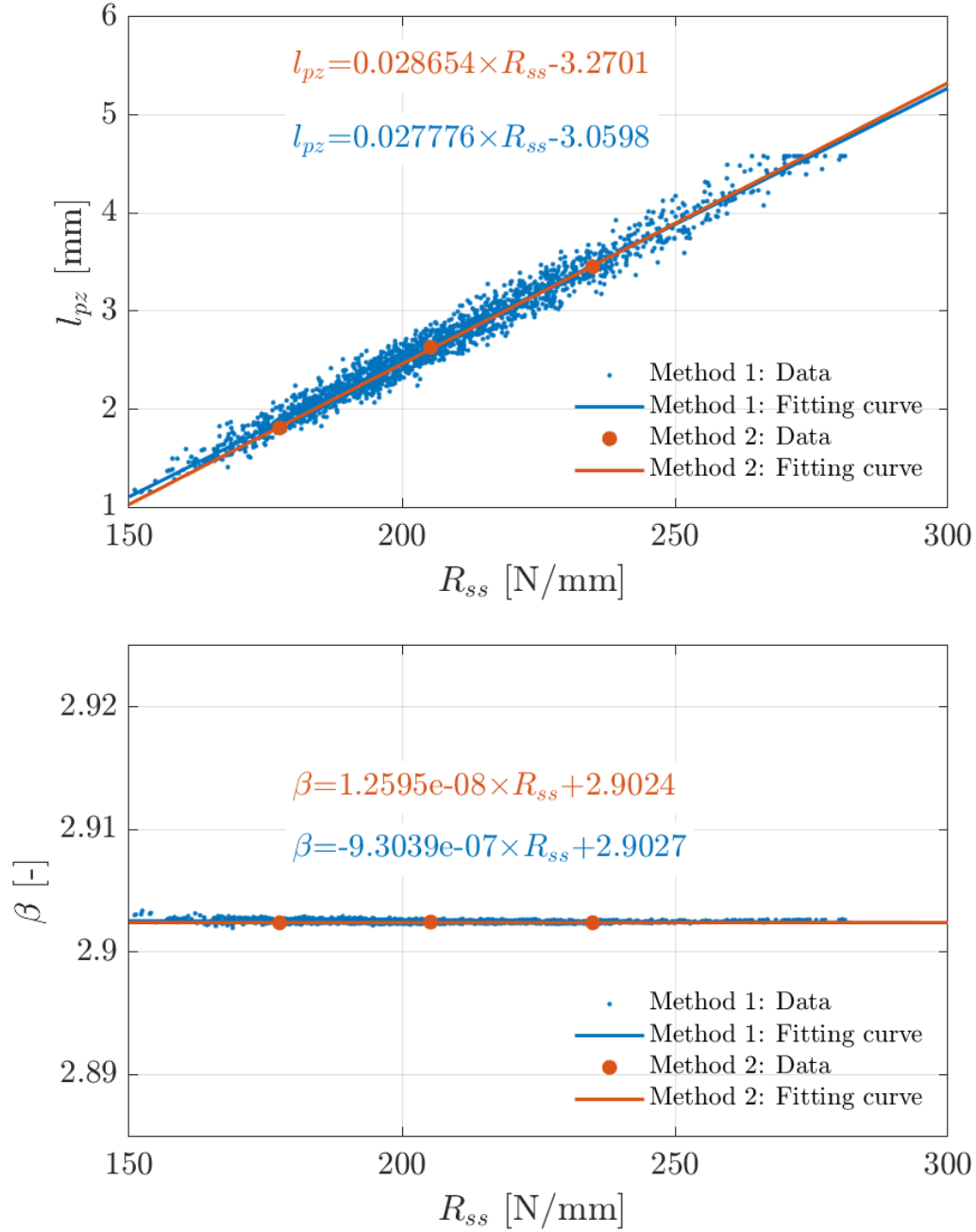


**Figure 5:**  $l_{f_{pz}} = f(\mathcal{R}_{ss})$  (top) and  $\beta = g(\mathcal{R}_{ss})$  (bottom) obtained with method 1 and method 2.

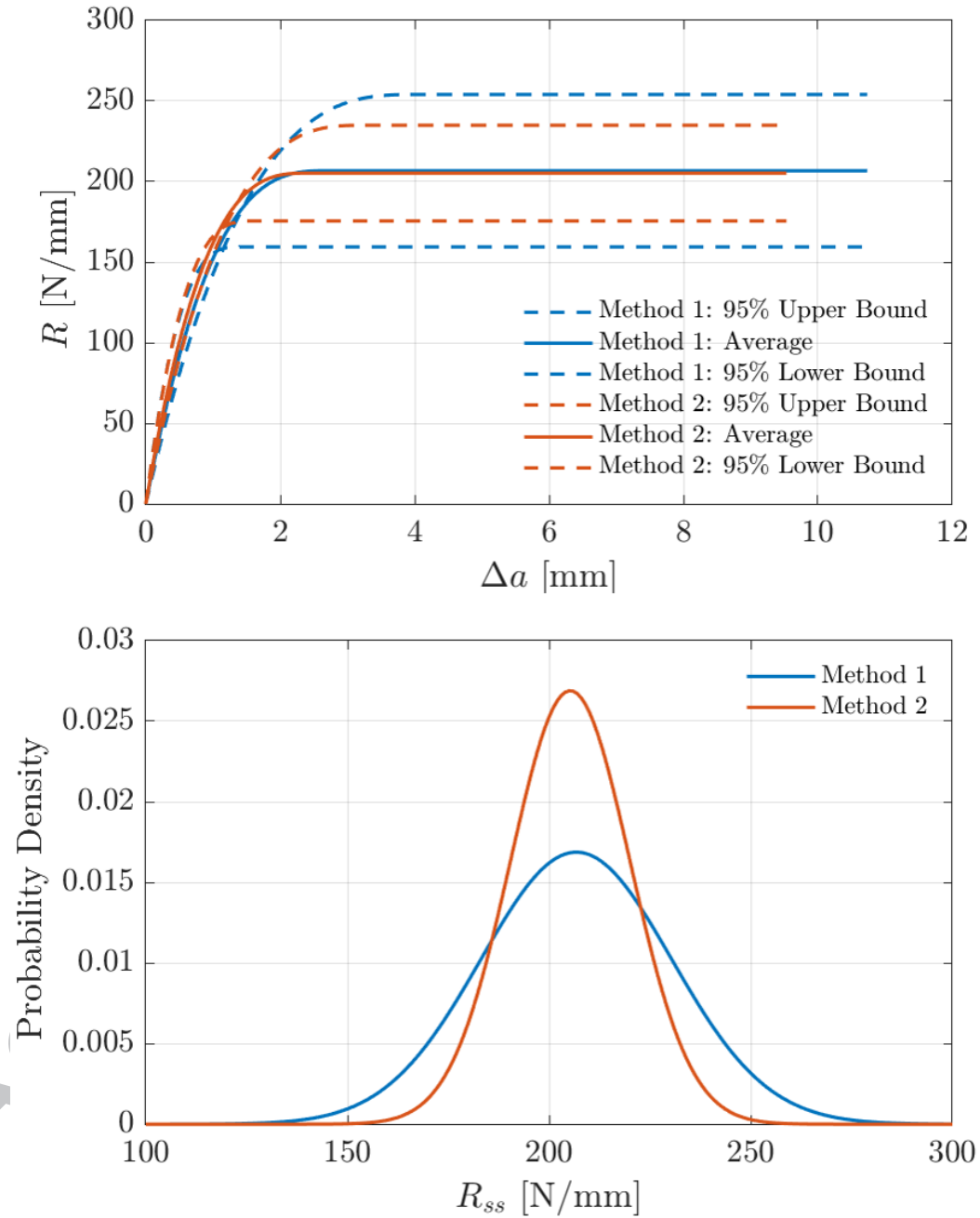


**Figure 6:** Average and 95% confidence bounds  $\mathcal{R}$ -curves (top) and predicted normal distribution of  $\mathcal{R}_{ss}$  using method 1 and method 2 (bottom).

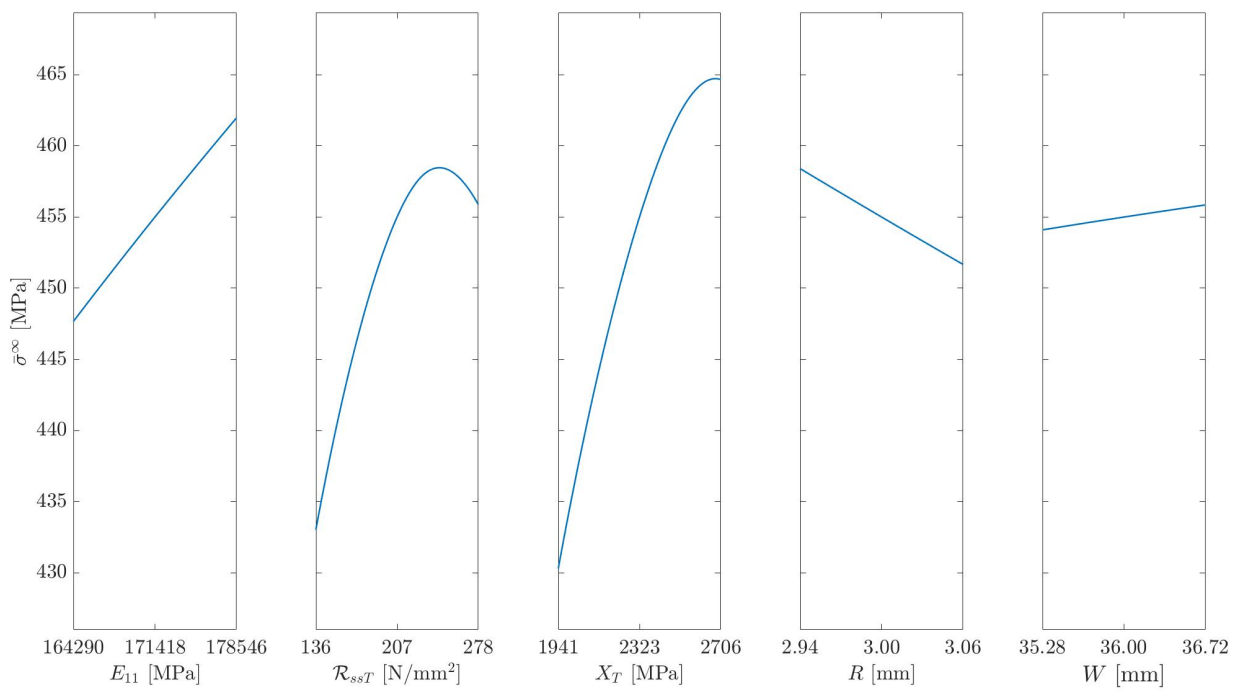


**Figure 7:** Sensitivity analysis on the notched strength for  $W = 36$  mm and  $R = 3$  mm.

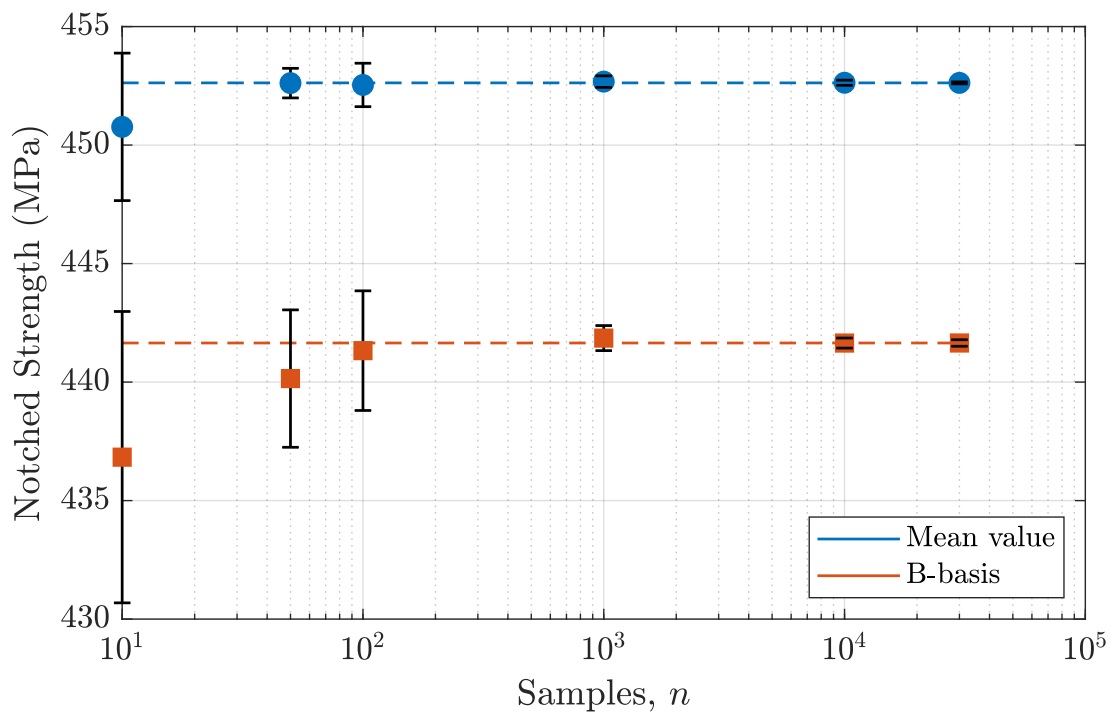


**Figure 8:** Average OH strength and 10th percentile from  $N = 10$  simulations determined from different number of samples  $n$ .

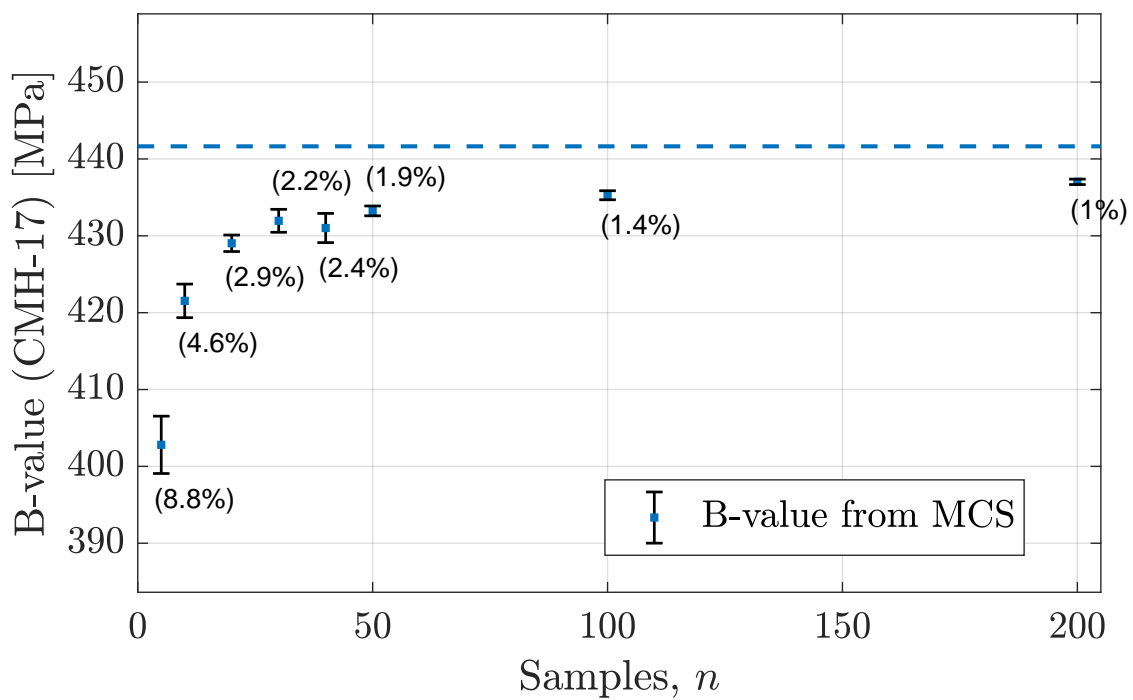


**Figure 9:** Comparison of the b-value obtained from the CMH-17 approach with its 95% interval of confidence, for different sample sizes ( $n$ ) and the B-value obtained from MCS (dashed line).

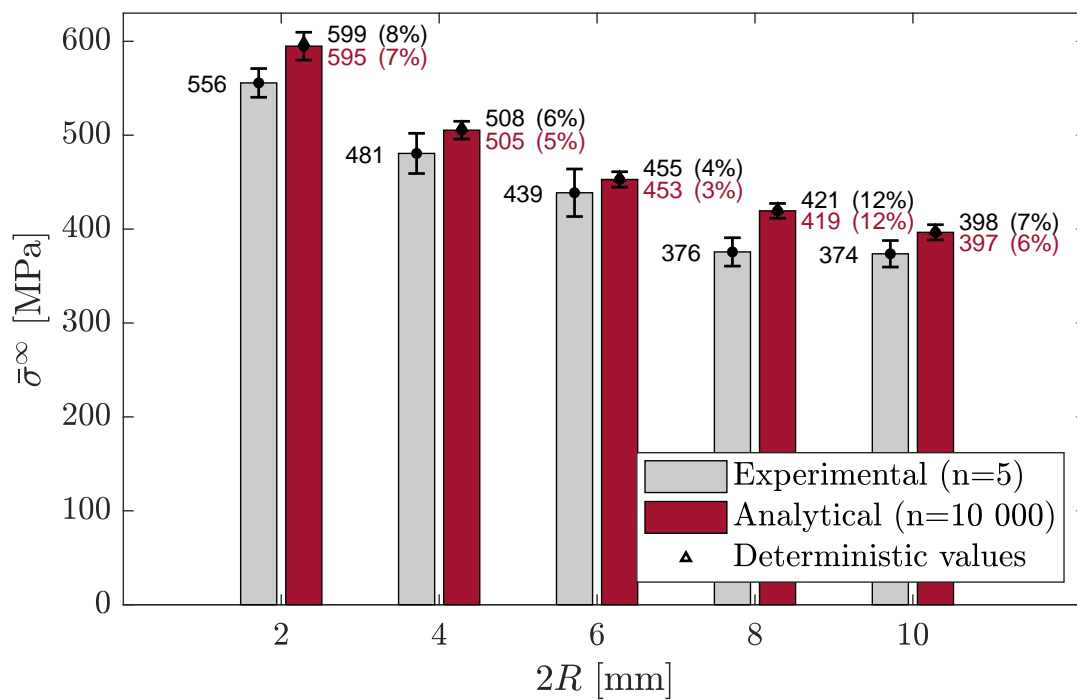


**Figure 10:** Comparison between the mean open hole strength of experimental results [18] and the analytical results of five different  $2R$  and a fixed ratio  $2R/W = 1/6$ , where  $\bar{\sigma}^\infty$  is the notched strength,  $R$  the radius of the hole and  $W$  the width.

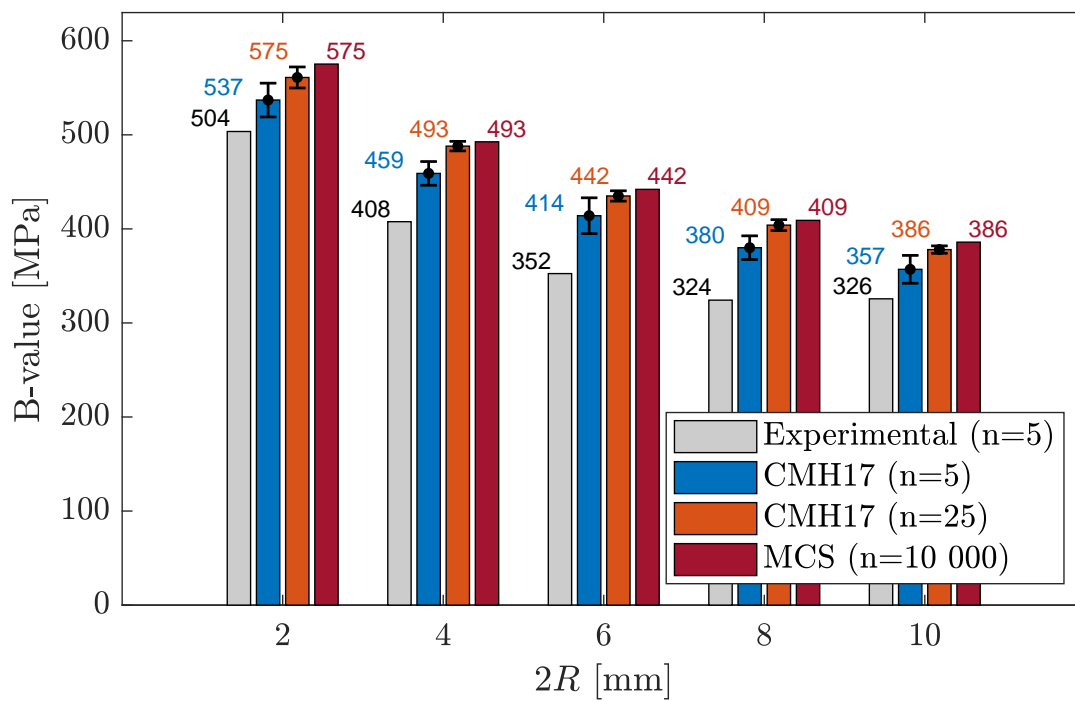


**Figure 11:** Comparison between the B-value obtained experimentally ( $n = 5$ ), with the CMH-17 ( $n = 5$  and  $n = 25$ ) and with the MCS method ( $n = 10,000$ ).

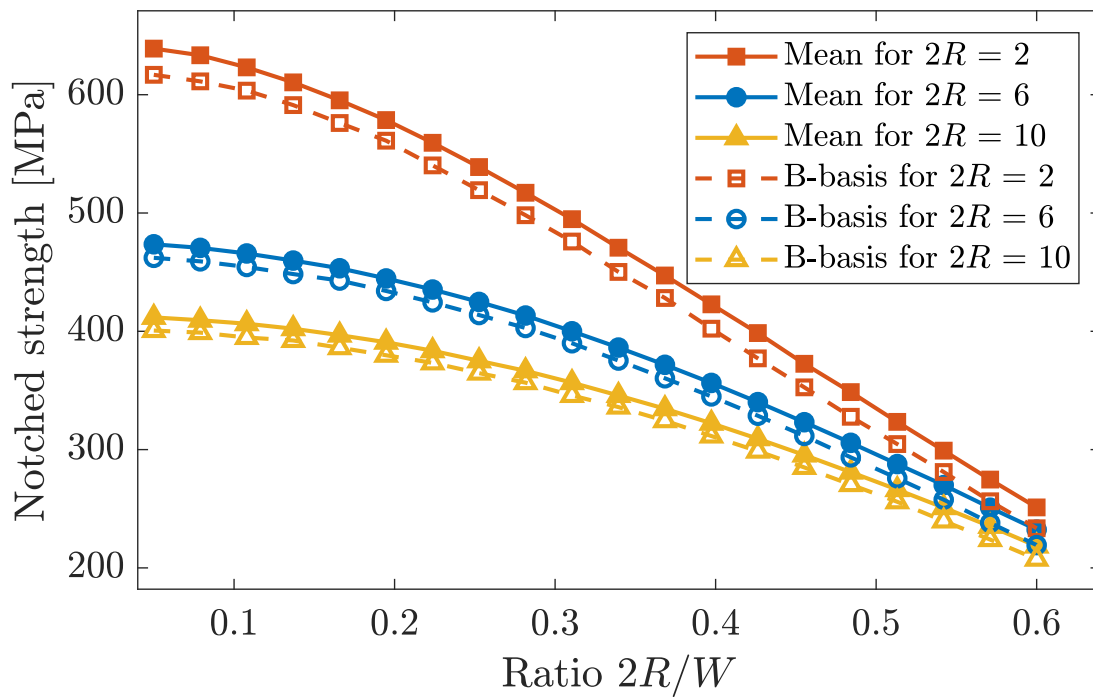


**Figure 12:** Design chart of the mean and B-basis value of the open hole strength calculated by means of MCS for different  $2R$  and  $2R/W$  ratios.



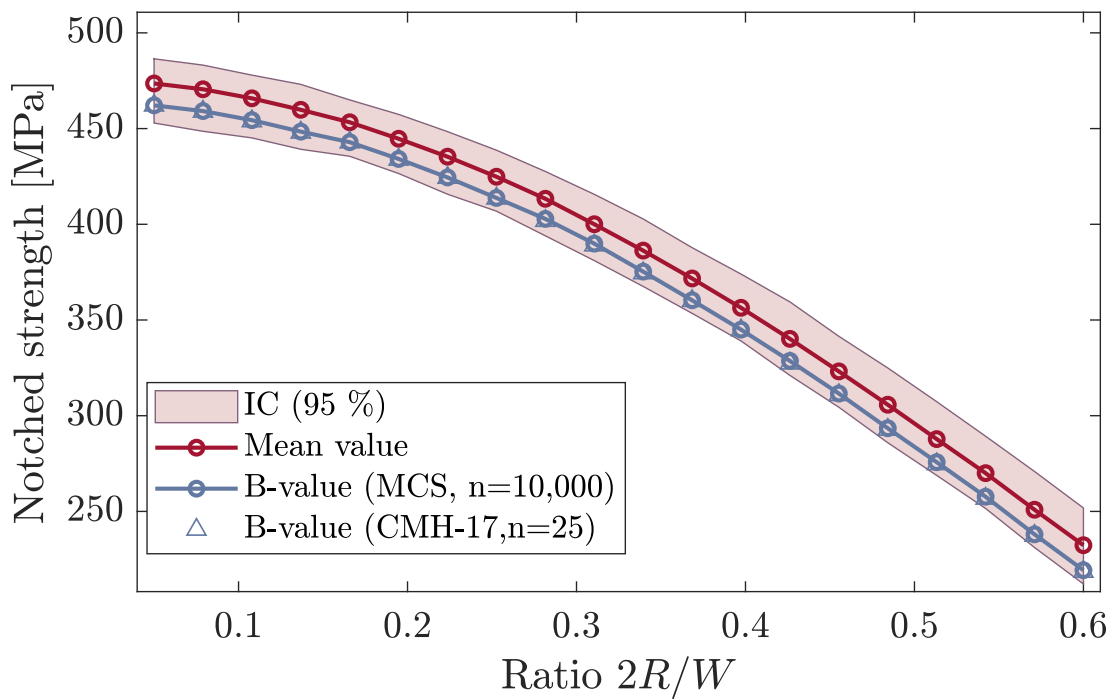


Figure 13: Design chart of the notched strength for  $2R = 6$  mm.

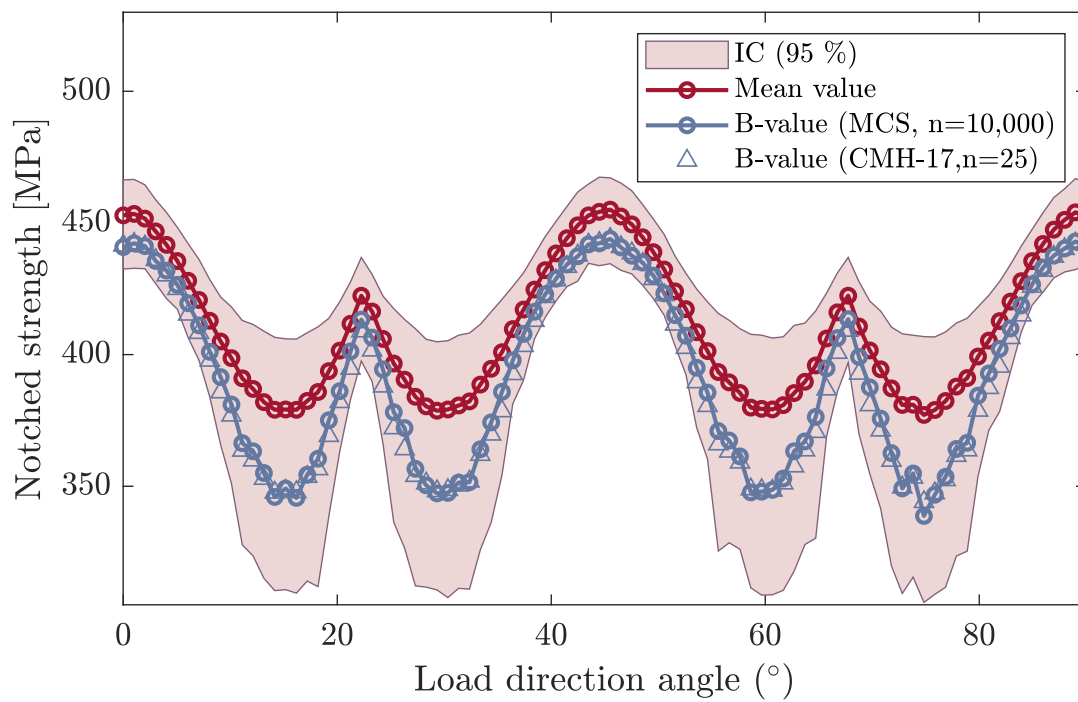


Figure 14: Notched strength variation with the load direction.

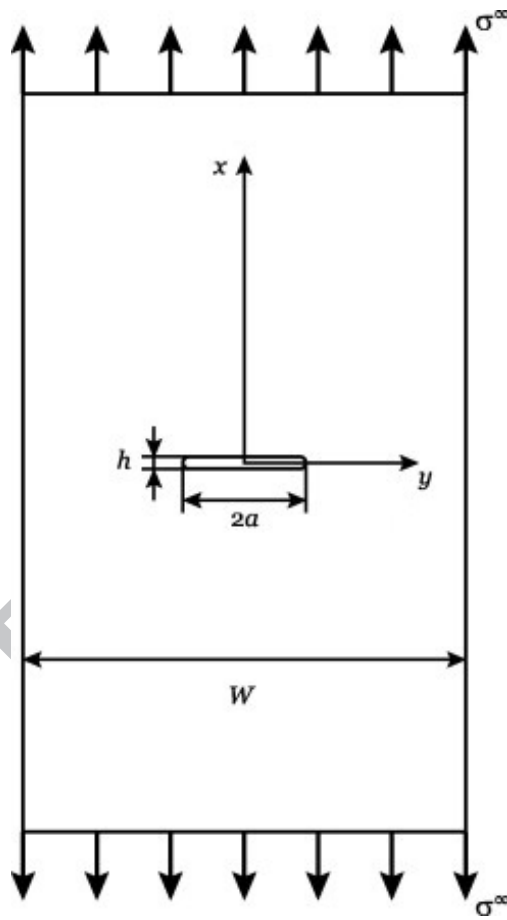
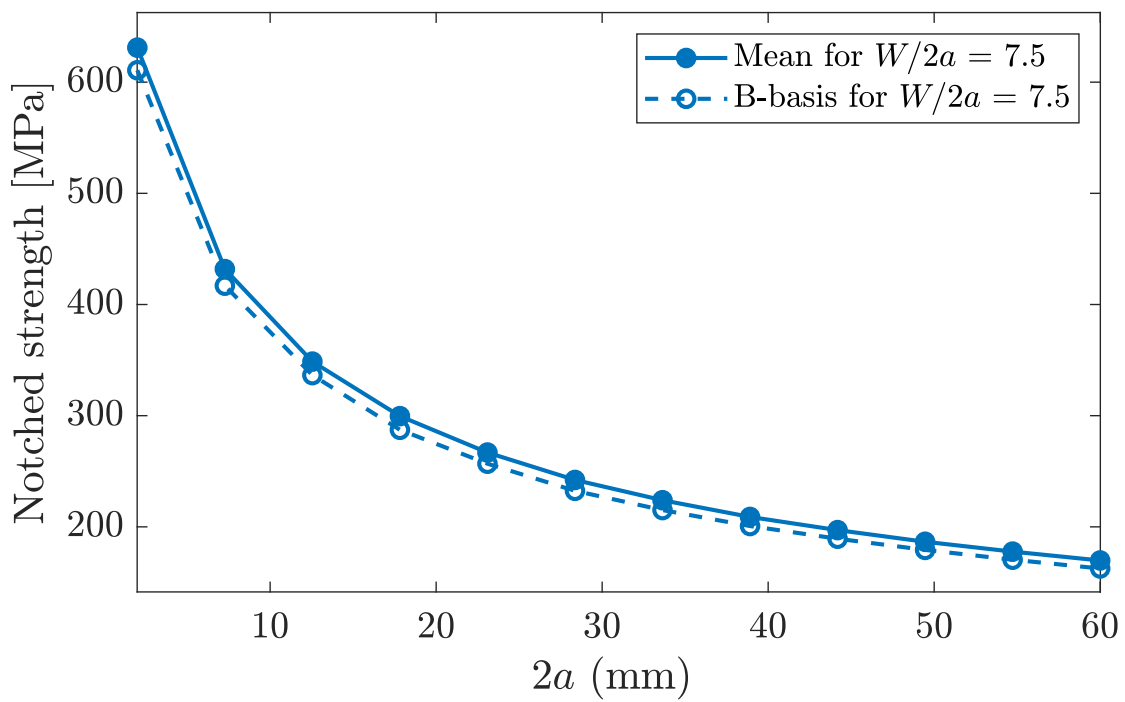


Figure 15: Centre notched plate configuration [19].



**Figure 16:** Design chart of the mean and B-basis value of the notched strength calculated by means of MCS ( $n = 10,000$ ) for centre notched plates.